

Ageing is important: Closing the fouling-cleaning loop

Edward M. Ishiyama^{1,2}, William R. Paterson² and D. Ian Wilson²

¹IHS Downstream Research, 133 Houndsditch, London EC3A 7BX, United Kingdom

²Department of Chemical Engineering and Biotechnology, New Museums Site, Pembroke Street, Cambridge
CB2 3RA, University of Cambridge, United Kingdom

Address correspondence to
Dr. D. Ian Wilson,
Department of Chemical Engineering and Biotechnology,
University of Cambridge,
New Museums Site,
CB2 3RA
Cambridge, UK.

E-mail: diw11@cam.ac.uk

Phone Number: 0 (+44) 1223 334 791, Fax Number: 0 (+44) 1223 334 796

ABSTRACT

Process units subject to fouling often require regular cleaning, giving rise to repeated cycles of fouling and cleaning. The initial stages of fouling are strongly influenced by the effectiveness of the most recent cleaning step and, similarly, the effectiveness and rate of cleaning is determined by the extent and nature of the deposit layer present on the surface. The optimal operating cycle will therefore be determined by fouling-cleaning interactions. Deposit ageing is an important factor in this, as an aged deposit is usually more difficult to clean. Ageing therefore introduces an element of choice into fouling-cleaning operating cycles, between in-situ 'chemical' methods and ex-situ 'mechanical' methods, with associated differences in effectiveness, time and cost. This paper reports a reformulation of the cleaning scheduling problem to consider the *choice* of cleaning method as well as the *timing* of cleaning. A case study based on a shell-and-tube heat exchanger processing crude oil is used to illustrate the concepts and scope of application of this approach. A novel and more general formulation of the problem, linking design, fouling and cost aspects via dimensionless groups is then presented and illustrated with a second case study based on a simpler exchanger model.

INTRODUCTION

Fouling-cleaning operating cycles arise from the regular cleaning of fouled process heat exchangers. Identification of the optimal operating period for an isolated exchanger subject to recurring fouling was first considered by Ma and Epstein [1]. The scheduling of heat exchanger cleaning operations has been considered since by many researchers, both for individual units (e.g. [2 - 3]) and for networks of exchangers (e.g. [4 - 7]). These analyses assumed that the cleaning action removes the whole deposit layer, so that the unit starts at the clean state when it is returned to operation. This is not always achieved in practice, particularly when a less aggressive cleaning method is employed. There are often several technologies available in practice, differing in terms of effectiveness, downtime and cost [8]. A choice then arises between a quick, less effective method and a rigorous but time-consuming alternative. An example from an oil refinery is the use of re-circulating solvent to wash away the bulk of a fouling layer, which requires units to be isolated but not dismantled, compared to water-jet blasting or pigging of tube bundles at remote locations. The former is an example of cleaning-in-place (CIP), which we label 'chemical' cleaning, while the latter is here termed 'mechanical' cleaning.

It is acknowledged that CIP, particularly as practiced in the food industry, can achieve complete removal of deposit. It is recognized that cleaning methods vary noticeably between industries and applications. For instance, CIP is widely practised in the food sector as it avoids exposing process surfaces to the air and thereby inviting contamination. Likewise, pigging and water jetting are widely practised in other sectors where the fouling deposits cannot be removed by other means.

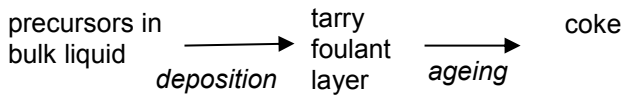
The selection of cleaning methods is determined by the nature of the fouling layer which is, in turn, governed both by the deposition mechanism and subsequent ageing. Figure 1 shows a modified schematic of the 'fouling-cleaning symbiosis' cycle presented by Wilson [9]. The initial stages of deposition are strongly influenced by the effectiveness of the most recent cleaning step and, similarly, the effectiveness and rate of cleaning are determined by the extent and nature of the fouling layer present on the surface. The choice of cleaning method and optimal operating cycle will therefore be determined by fouling-ageing-cleaning interactions. In crude oil fouling, the freshly deposited material often takes the form of a gel, which over time converts to a harder, 'coke' layer. The former may be removed by solvent washing, but the latter requires the unit to be isolated and dismantled for mechanical cleaning. Ageing therefore introduces a systematic factor into the choice of fouling-cleaning operating cycles, between in-situ 'chemical' methods and ex-situ 'mechanical' methods, with associated differences in effectiveness, time and cost. This requires a reformulation of the problem from that set out by Ma and Epstein [1], and was first presented by Ishiyama *et al.* [10], who illustrated the concept with a case study based on an evaporator. The numerical aspects of the associated optimisation problem, on 'how' and 'when' to clean a unit, were further investigated by Pogiatis *et al.* [11], in which a comparison of a heuristic approach and a NLP (non-linear programming) based approach is given.

In this paper, a mathematical formulation for identifying optimal cleaning cycles is presented. Its application is initially demonstrated by a case study employing a detailed heat exchanger model. The choice of models to describe ageing is discussed briefly, summarising some of our recent work in this area. The formulation is then extended to a more general case, which yields a set of dimensionless groups that draw together the key factors

involved. The formulation is then extended to situations where ageing gives rise to a choice of cleaning actions. The importance of ageing, and its impact on cleaning decisions, is demonstrated with a case study for an idealised single pass shell-and-tube heat exchanger. A basic two-layer model is employed to describe ageing in terms of heat transfer and ease of removal as this simplifies the calculations, but the approach is generic and readily extendable to other models.

Describing ageing: the two-layer model

Ageing is modelled here as the fouling deposit undergoing conversion between two forms, termed gel and coke, being a development of the concept proposed by Crittenden and Kolackowski [12]. The deposit is modelled as two sub-layers: the coke represents that part of the deposit that cannot be removed by quick ('chemical') methods.



The two-layer model is employed here as a simplification of ageing in real systems, which involves complex and largely non-quantified chemistry [13]. It represents the simplest quantitative treatment of the evolution of a deposit layer from freshly deposited material, deemed to be susceptible to chemical cleaning, to coke, which cannot be removed by a chemical clean.

The micro-structural changes associated with deposit hardening during ageing not only modify the rheology of the deposit but also, normally, increase its thermal conductivity, λ . Ageing therefore couples thermal, fouling and cleaning performance: λ determines the temperature distribution within the deposit (and local ageing rate) as well as the deposit-liquid interface temperature (and deposition rate). Ishiyama *et al.* [14] presented a quantitative distributed model of deposit ageing and used it to investigate the impact of ageing on chemical reaction fouling behaviour. They used a fouling model and parameter values for crude oil fouling and compared the effect of ageing on results obtained under typical laboratory test conditions with plant operating modes. They modelled the thermal conductivity as changing continuously from the initial gel (soft material) value, λ_g , to that of coke (hard material), λ_c , using a simple kinetic scheme (see Figure 2 (a)). They did not consider the impact of ageing on cleaning.

In this paper we assume that the thermal conductivity of the deposit layer may be modelled using the simple two-layer model, shown in Figure 2 (b). The analysis also assumes that the deposit density remains constant. This may not be a valid assumption if thermal cracking becomes important. The overall thickness of the deposit, δ , is given by the sum of the gel and coke sub-layer thicknesses:

$$\delta = \delta_g + \delta_c \quad (1)$$

In the absence of experimental data, and to simplify the mathematics, we assume that the overall fouling resistance of the deposit, R_f , is given by

$$R_f = \frac{\delta_g}{\lambda_g} + \frac{\delta_c}{\lambda_c} \quad (2)$$

This represents an intrinsic linking of cleaning behaviour (equation (1)) and thermal performance (equation (2)) via the sub-layer thicknesses. In practice the division between rheological and thermal properties may lie at different points, which could be modelled using a distributed thermal model [14]. The simple (linked) model is used here as our aim is primarily to illustrate the concept.

Before the two-layer model is employed in cleaning scheduling, the kinetics of the gel-coke evolution need to be represented. Ishiyama et al. [15] established the most appropriate kinetic scheme to use by comparing the R_f -time results from their distributed model with two simple cases, namely a zeroth order and a first order kinetic scheme. Both schemes employed the following equations of change, based on equations (1) and (2):

$$\dot{\delta}_g = r_d - r_c \quad (3)$$

$$\dot{\delta}_c = r_c \quad (4)$$

Giving

$$\dot{R}_f = \frac{1}{\lambda_g}(r_d - r_c) + \frac{1}{\lambda_c}r_c \quad (5)$$

Here r_d is the deposition rate and r_c the rate of conversion to coke, both written as velocities. The deposition rate employs a simplified expression for tube-side chemical reaction fouling (more complex models could be used as desired):

$$r_d = \lambda_g a_d Re^{-0.8} Pr^{-0.33} \exp\left(\frac{-E_d}{RT_s}\right) \quad (6)$$

Here, Re and Pr are the Reynolds number and Prandtl numbers of the bulk liquid, respectively; T_s is the temperature at the deposit(gel)–liquid interface, *i.e.* in contact with the flowing fluid, R is the gas constant, E_d is the activation energy for deposition and a_d is a pre-exponential factor dictating the time-scale of deposition. A single value of E_d , namely 50 kJ mol^{-1} , was considered, which is representative of temperature sensitivities reported in the literature [16]. Different activation energies were considered for the ageing step, r_c , so that the effect of temperature sensitivity on ageing was isolated from its effect on deposition.

Zeroth order ageing (Model 0)

The coke layer is assumed to grow as a front, with the rate of growth determined by the temperature at the sub-layer interface, T_{int} .

$$r_c = \begin{cases} k_0 & \text{when } \delta_g > 0 \\ 0 & \text{when } \delta_g = 0 \end{cases} \quad (7)$$

where the rate constant k_0 is given by

$$k_0 = a_0 \exp\left(\frac{-E_0}{RT_{\text{int}}}\right) \quad (8)$$

First order ageing (Model I)

The rate of growth of the coke layer is related to the amount of gel present. A simple physical interpretation of this model is not available but it avoids the bifurcation in equation (7) and proves to be mathematically similar to the distributed model in certain cases. This gives

$$r_c = k_1 \delta_g = a_1 \exp\left(\frac{-E_1}{RT_{\text{int}}}\right) \delta_g \quad (9)$$

Both kinetic schemes require T_{int} to be evaluated, which required solution of the associated heat transfer problem, including curvature and changes in Re with deposit thickness.

Distributed ageing model (Model II)

This is described in detail in [14]. The rate of ageing is described by the first order decay of a localized structural variable, whose temperature sensitivity is quantified by the activation energy E_{II} .

The deposition model (Equation (6)) and the above ageing models (0-II) all employ Arrhenius-type kinetic schemes, which must be replaced by more reliable forms where possible. For instance, several studies on crude oil fouling report significant levels of inorganic material, particularly FeS, and these materials will undergo different reaction and ageing pathways to hydrocarbon only materials. For example, Derakshesh *et al.* [17] reported appreciable levels of FeS in deposits under coking conditions and the development of a porous deposit at higher temperatures, which is attributed to subcooled boiling.

COMPARISON OF AGEING MODELS

The zeroth and first order ageing models described above present readily tractable forms suitable for optimization calculations on the scheduling problem. Their suitability was tested by comparison with Ishiyama *et al.*'s [14] distributed model over a range of conditions, where the latter was assumed to predict the true thermal effect of ageing. The test vehicle was a typical heat exchanger tube (nominal one inch, i.d. 0.0229 m) with a medium viscosity crude oil at 270 °C (518°F) flowing at 0.3 kg s⁻¹ (clean velocity ~1 m s⁻¹) on the tube-side. The values of Re and Pr were ~ 40,000 and ~ 9.5, respectively. Other parameter values were: $a_d = 1 \times 10^5 \text{ m}^2\text{K kW}^{-1} \text{ h}^{-1}$, $\lambda_g = 0.1 \text{ W m}^{-1}\text{K}^{-1}$, $\lambda_c = 1.0 \text{ W m}^{-1}\text{K}^{-1}$. Further details of the simulations are given in 14. Two primary parameters were investigated:

(i) Ageing activation energy

The activation energy for deposition, E_d , was kept constant at 50 kJ mol⁻¹. The effect of different ageing temperature sensitivity was studied by considering ageing activation energies of 10, 50 and 200 kJ mol⁻¹. In order to compensate for the difference in activation energies, the ageing pre-factor a_i was adjusted to give the same initial ageing rate via:

$$a_{i,E_j} = a_{i,10 \text{ kJ mol}^{-1}} \exp\left(-\frac{10,000 - E_j}{RT_s}\right) \quad (10)$$

where the value of T_s used is that in the initial (usually clean) condition.

(ii) Relative rates of deposition and ageing

When ageing is rapid compared to the rate of gel deposition, the gel layer thickness approaches zero and the deposit takes the form of a coke sub-layer. Likewise, slow ageing means that the deposit behaves as if it were a gel sub-layer. Three scenarios were investigated, namely slow ageing with respect to deposition; medium ageing, and fast ageing. The a_i values used are given in Table 1.

Figure 3 shows the results obtained for the case of slow ageing when operating at constant heat flux, which is the mode employed in many experimental fouling tests. The plots all show a decrease in thermal fouling rate caused by the conversion of gel to coke (and decrease in deposit thermal resistance). Linear fouling would be observed in the absence of ageing as the gel-liquid interface temperature does not change noticeably. The absence of ageing could also arise if the deposit contained an appreciable amount of inorganic material as this will not change over time. Also shown in Figure 3(a) is a relative time scale, t^* , where $t^* = 1$ indicates the time taken for the tube-side heat transfer coefficient to decrease to half its initial value (fouling Biot number = 1).

The plots show that the agreement between each of the two-layer models and Model II varies, depending on the relative rate of ageing and temperature sensitivity. The summary of the agreement observed across all nine scenarios in Table 2 indicates that Model I provided a satisfactory shortcut description for all cases. Model 0 could be used to describe cases with rapid ageing or high temperature sensitivity.

The corresponding plots for operation at constant wall temperature are presented in Figure 4. The non-ageing reference case exhibits falling rate fouling behaviour owing to the change in gel-liquid interface temperature. The summary in Table 3 includes some important differences from Table 2, in that neither two-layer model provided a good approximation to the distributed model for scenarios with strong temperature sensitivity, and, interestingly, for the case of medium ageing rate (Figure 3b, Figure 4b) and mid-range temperature sensitivity. In the absence of supporting information, the first order kinetic model appears to offer a more robust description of ageing at this coarse level of scrutiny, notwithstanding the lack of a physical justification of its mathematical form. Experimental data supporting the choice of either model would be highly desirable.

In the following sections the first order kinetic scheme [Model I] is used to describe ageing in a case study for a particular exchanger. The zeroth order kinetic scheme [Model 0] is used in the generalised formulation for its mathematical simplicity as the purpose of that work is to illustrate concepts.

SCHEDULING WITH CHOICE: SUPER-CYCLES

Fouling causes reduced heat transfer efficiency, and thermal performance is used here to construct a cost function for the scheduling algorithm. The effect of fouling on throughput and pressure drop is not considered but could be incorporated if required. The impact on chemical and mechanical cleaning on fouling and the heat duty of an exchanger, Q , is shown schematically in Figure 5. Linear deposit growth kinetics are employed for illustration.

Identifying a cleaning schedule requires selection of cleaning method (chemical or mechanical) and time of cleaning (t_M , t_C). The choice of cleaning method introduces two dimensionless ratios, namely

$C_{cl,C} / C_{cl,M}$ ratio of cleaning costs ($C_{cl,C}$ and $C_{cl,M}$ are the cost of chemical and mechanical cleaning actions, respectively)

τ_C / τ_M ratio of cleaning period lengths (τ_C and τ_M are the time taken for chemical and mechanical cleaning actions, respectively)

Both ratios are expected to be < 1 in order to offset the poorer cleaning performance expected for chemical cleaning.

Figure 5(b) shows that chemical cleaning results in an increase in heat duty when the unit is returned to operation but that the decay caused by fouling continues. Mechanical cleaning, however, restores the unit to its clean state and effectively restarts the process. The period between each mechanical clean, which can include any number of chemical cleans, is repeated if the parameters remain constant: this is termed the 'super-cycle' and the identification of a super-cycle with the lowest time-averaged cost is the objective for the scheduling problem.

It should be noted that the impact of different cleaning methods on fouling induction periods has not been considered here but could be introduced readily. Chemical cleaning is deemed to leave a residual foulant layer on which deposition is likely to start soon after the unit is returned to service, whereas a mechanically cleaned surface may require conditioning (i.e. an induction period) before deposit can attach and grow.

The objective function is written in terms of cost, with three components:

- (i) Cost of additional heating, provided elsewhere in the process, to compensate for the loss in heat transfer in the exchanger due to fouling

$$C_E \int_0^t (Q_{cl} - Q) dt \quad (11)$$

Here, C_E is the cost of energy and Q_{cl} is the heat duty of the exchanger in the clean state.

- (ii) Additional heating costs during the period when the exchanger is taken off-line for cleaning,

$$C_E Q_{cl,C} \tau_C \text{ or } C_E Q_{cl,M} \tau_M$$

for chemical or mechanical cleaning, respectively.

(iii) Cost of each cleaning action; $C_{cl,C}$ or $C_{cl,M}$.

These costs are then summed and the total averaged loss, TAL , calculated from

$$TAL = \frac{\left(C_E \int_0^{t_M} (Q_{cl} - Q(t')) dt + N_C (C_{cl,C} + Q_{cl} \tau_C) + C_{cl,M} Q_{cl} \tau_M \right)}{t_{cycle} = t_M + \tau_M} \quad (12)$$

where N_C is the number of chemical cleaning actions between each mechanical clean.

The aim of the scheduling calculation is to minimise TAL subject to various constraints. There are several approaches for generating solutions to this problem, and a relatively simple method is employed here. A stepwise marching algorithm is used to evaluate the best local decision (lowest cost) of available options. Chemical cleaning is favoured if it gives TAL lower than that given by mechanical cleaning at that point in time. Cleaning is then performed and the algorithm moves on to the next period, until mechanical cleaning resets the process [10-11].

Cleaning super-cycle case study for a shell-and-tube heat exchanger

Ishiyama *et al.* [10] considered optimizing chemical and mechanical cleaning for an evaporator with fixed temperature driving force. The case considered here involves sensible heat transfer in a counter-current heat exchanger. The unit is a single segmental baffled, shell-and-tube unit with crude flowing on the tube-side. In the clean state the crude temperature increases from 220°C to 237°C, corresponding to a clean heat duty of 11.7 MW. The physical properties of the process streams are summarized in Table 4, while design and initial operating parameters are given in Table 5. Deposition (gel formation) is modelled using equation (6) with $a_d = 36 \text{ m}^2\text{K kW}^{-1} \text{ h}^{-1}$ and $E_d = 50 \text{ kJ mol}^{-1} \text{ K}^{-1}$. Ageing of the deposit described by equation 9 (first order model) with $E_1 = 50 \text{ kJ mol}^{-1} \text{ K}^{-1}$. a_1 values of 100, 500 and 1000 day^{-1} are considered here.

Figure 6(a) shows the overall fouling resistance-time profiles for different rates of ageing (varying a_1) while Figure 6(b) compares the deposit thickness reached after 1000 days of operation. Fouling in all cases causes a significant reduction in the overall heat transfer coefficient. This is not matched by the deposit thickness, however: ageing actually results in a slightly larger total amount of deposit. This occurs because the increase in overall thermal conductivity with ageing reduces the overall fouling resistance, so that the deposit surface temperature is higher, promoting deposition. The growth of the coke layer with increasing a_1 is evident.

The results in Figure 6 assume that the fouling rate is uniform over the heat transfer surface, both circumferentially and along its length. In practice there will be a variation in film and surface temperatures across the unit, which will give rise to differences in deposition and ageing rates with position if these processes are strongly temperature sensitive or the temperatures vary by a large extent. Ishiyama *et al.* [18] presented an analytical result for the overall fouling rate for units with a linear temperature profile exhibiting kinetic forms similar to Equation (6). Numerical simulation is required when temperature-dependent ageing occurs, as reported by Coletti *et al.* [19].

The cleaning super-cycle algorithm described above was used to identify optimal combinations of chemical and mechanical cleaning actions for different costing scenarios. Figure 7 shows the results from one scenario, where two chemical cleaning operations are performed for each mechanical one, giving a super-cycle period of ~850 days. The *residual* fouling resistance following chemical cleaning actions is evident, and the amount does not follow a linear trend.

The influence of different cost and cleaning time ratios on super-cycle and TAL for $a_1 = 500 \text{ day}^{-1}$ is summarized in Figure 8. Figure 8(a) shows that the length of the super-cycle (and number of chemical cleaning actions) increases with increase in mechanical cleaning parameters ($C_{cl,M}$ and τ_M). The number of solvent cleaning actions in each optimised super-cycle is marked on Figure 8(a). As a discrete action, solvent cleaning gives rise to a series of steps in the solution plane. The Figure shows that more chemical cleans are employed as mechanical cleaning becomes less attractive, which is the expected tendency.

The mixed cleaning strategy can be compared with one based solely on mechanical cleaning. The optimization problem is similar to that considered by Casado [2] and the results for this case are plotted as a continuous plane on Figure 8(b). The plot demonstrates that a mixed cleaning strategy is always economically more attractive for the

parameter set considered here. As a_1 increases and the effectiveness of chemical cleaning decreases, mechanical cleaning is likely to become more attractive and eventually be favoured over a mixed cleaning strategy.

A MORE GENERAL ANALYSIS OF OPTIMAL CLEANING CYCLES IN THE ABSENCE OF DEPOSIT AGEING

The above case study considered a specific heat exchanger with set configuration and operating conditions. The influence of exchanger design parameters was not considered, even though these will affect the unit's response to fouling and the rate of deposition (*via*, for instance, the surface temperatures in the unit).

A more general analysis is now presented which reduces certain aspects of heat exchanger design and performance to simple relationships so that the inter-relationships can be explored and general lessons extracted. Detailed modelling is required for more precise results: the aim of this analysis is to construct a framework for mapping out the solution landscape. In this first part we suppress all considerations of ageing, in order to establish the general landscape.

The analysis considers an isolated heat exchanger, with a simple configuration, namely a pure counter-current unit with equal heat capacity flow rates, *i.e.* $W_{\text{hot}} = W_{\text{cold}}$, where W_j is the heat capacity flow rate of stream j . A formulation for determining the optimal cleaning cycle is constructed for the case of mechanical cleaning only, and then extended to include chemical and mechanical cleaning.

Heat transfer and fouling

Assuming negligible changes in surface roughness and film transfer coefficients as deposition proceeds, the contribution of the foulant layer to the overall thermal resistance is given by

$$\frac{1}{U} = \frac{1}{U_{\text{cl}}} + R_f \quad (13)$$

where U_{cl} is the overall heat transfer coefficient in the clean state and U is the 'dirty' value. If the rate of increase in fouling resistance, $\dot{R}_{f,\text{total}}$, is constant, equation (13) can be rewritten as

$$\frac{1}{U} = \frac{1}{U_{\text{cl}}} + \dot{R}_{f,\text{total}} t \quad (14)$$

Equation (2) can be written as

$$U = \frac{a_1}{a_2 + t} \quad (15)$$

where a_1 and a_2 are dimensional constants: $a_1 = (1/\dot{R}_{f,\text{total}})$ and $a_2 = 1/(U_{\text{cl}}\dot{R}_{f,\text{total}})$.

The performance of the heat exchanger is related to the number of transfer units, NTU ,

$$NTU = \frac{UA}{W_{\min}} = \frac{a_1 A}{(a_2 + t)W_{\min}} \quad (16)$$

where A is the surface area for heat transfer and W_{\min} is the smaller of the two heat capacity flow rates. For a counter current exchanger with $W_{\text{hot}} = W_{\text{cold}} = W_{\min}$, the effectiveness, ε , is given by

$$\varepsilon = \frac{NTU}{1 + NTU} \quad (17)$$

The effectiveness relates the actual heat duty, Q , to the thermodynamically maximum possible duty, Q_{\max} , via:

$$Q = \varepsilon Q_{\max} = \varepsilon W_{\min} DT_{\max} \quad (18)$$

where DT_{\max} is the maximum achievable temperature change, given by $T_{\text{hot,inlet}} - T_{\text{cold,inlet}}$.

Combining (16) and (17) gives

$$\varepsilon = \frac{a_1 A}{(a_2 + t)W_{\min} + a_1 A} \quad (19)$$

The exchanger configuration used here (counter-current, with $W_{\text{hot}} = W_{\text{cold}}$) was selected to give a tractable analytical solution for the super-cycle formulation. The approach applies to any heat exchanger configuration, but numerical computation is likely to be required for generating the solutions.

Substituting (18) into (19) gives,

$$Q = \varepsilon Q_{\max} = \left[\frac{a_1 A}{(a_2 + t)W_{\min} + a_1 A} \right] W_{\min} DT_{\max} \quad (20)$$

$$Q = \frac{a_3}{(a_4 + t)} \quad (21)$$

Here,

$$a_3 = a_1 A DT_{\max} \quad (22)$$

$$a_4 = a_2 + \frac{a_1 A}{W_{\min}} \quad (23)$$

When a heat exchanger is operated for a time period of length t and then subject to cleaning for a cleaning period of τ_M , the daily averaged operational and maintenance cost, ϕ , based on equation (13) is

$$\phi = \frac{C_E \left[\int_0^t (Q_{\text{cl}} - Q) dt + Q_{\text{cl}} \tau_M \right] + C_{\text{cl},M}}{t + \tau_M} \quad (24)$$

Here, C_E is the cost of energy, Q_{cl} is the clean heat duty, $C_{\text{cl},M}$ is the cleaning cost (mechanical cleaning), and τ_M is the mechanical cleaning time.

Evaluation of $\int_0^t (Q_{\text{cl}} - Q) dt$ when $Q = \frac{a_3}{a_4 + t}$ gives

$$\phi = \frac{C_E \left[Q_{\text{cl}} t - a_3 \ln \left| \frac{a_4 + t}{a_4} \right| + Q_{\text{cl}} \tau_M \right] + C_{\text{cl},M}}{t + \tau_M} \quad (25)$$

The time when ϕ is minimum, t_{opt} , is given by setting $\frac{d\phi}{dt} = 0$. It can be shown that the condition for a minimum, that $\frac{d^2\phi}{dt^2}$ is positive, also holds. Differentiating the RHS of equation (25) and substituting the identities a_1, a_2, a_3 and a_4 yields

$$Q_{cl}t_{opt} - \frac{ADT_{max}}{\dot{R}_f} \ln \left| \frac{\frac{1}{\dot{R}_f U_{cl}} + \frac{A}{\dot{R}_f C_{min+t_{opt}}}}{\frac{1}{\dot{R}_f U_{cl}} + \frac{A}{\dot{R}_f W_{min}}} \right| + Q_{cl}\tau_M + \frac{C_{cl,M}}{C_E} \quad (26)$$

This gives

$$1 + \frac{U_{cl}A}{W_{min} + \dot{R}_f U_{cl}}$$

Equation (27) is intentionally written in the form of ratios to emphasise that the optimal condition is determined by a series of competing factors. It is now subject to a dimensional analysis. There are ten variables, namely ($A, DT_{max}, \dot{R}_f, \tau_M, C_E, C_{cl}, Q_{cl}, U_{cl}, W_{min}, t_{opt}$), and five primary dimensions ([M], [L], [T], [t], [\$]). Buckingham's π theorem indicates that there should be five independent dimensionless groups.

Inspection of equation (27) yields the following five candidates (summarised in Table 6).

1. The clean NTU value, $\Pi_1 = U_{cl}A / W_{min}$, is determined by the detailed design of the exchanger. Together with Π_2 , it determines the performance of the exchanger and its sensitivity to fouling.
2. The clean effectiveness, $\Pi_2 = Q_{cl} / W_{min} DT_{max}$, which is determined by the process design.
3. A dimensionless fouling rate, $\Pi_3 = \dot{R}_f U_{cl} \tau_M$; τ_M is the only timescale specified in the problem.
4. A dimensionless cost, $\Pi_4 = C_{cl,M} / \tau_M Q_{cl} C_E$, which is the ratio of the costs incurred in cleaning the exchanger, being the cost of the cleaning action and the energy lost while the exchanger is out of service.
5. The optimal cleaning period, $\Pi_5 = t_{opt} / \tau_M$, which is the dimensionless value of the solution.

The objective function also yields an optimized cost, ϕ_{min} , which can be written as $\phi_{min} / C_E Q_{cl}$ ($=\Pi_6$)

Equation (27) can then be written

$$(\Pi_5 + 1) \left(1 - \frac{\frac{1}{\Pi_2}}{\frac{1}{\Pi_1} + 1 + \frac{\Pi_3 \Pi_5}{\Pi_1}} \right) = \left(\Pi_5 - \frac{\Pi_1}{\Pi_2 \Pi_3} \ln \left| \frac{1 + \Pi_1 + \Pi_3 \Pi_5}{1 + \Pi_1} \right| + 1 + \Pi_4 \right) \quad (28)$$

The associated minimum average daily cost, ϕ_{opt} , is given by

$$\phi_{\text{opt}} = \frac{C_E \left[Q_{\text{cl}} t_{\text{opt}} - E \ln \left| \frac{D + t_{\text{opt}}}{D} \right| + Q_{\text{cl}} \tau_M \right] + C_{\text{cl},M}}{t_{\text{opt}} + \tau_M} \quad (29)$$

or, in dimensionless terms

$$\Pi_6 = \frac{\left[\Pi_5 - \frac{\Pi_1}{\Pi_2 \Pi_3} \ln \left| \frac{1 + \Pi_1 + \Pi_3 \Pi_5}{1 + \Pi_1} \right| + 1 \right] + \Pi_4}{(\Pi_5 + 1)} \quad (30)$$

Illustration – mechanical cleaning only

The dimensionless formulation allows one to explore the characteristics of the solution space for an exchanger without being distracted by detail. Table 6 gives ranges of $\Pi_1 - \Pi_4$ for oil refinery preheat train exchangers with parameters based on the authors' experience. It must be emphasized that the parameter values will vary from one site to another, and between industrial sectors.

Let us consider a well-designed heat exchanger (from the point of view of thermal performance) with clean initial effectiveness of 0.9. It follows from equation [17] that $\Pi_1 = 9$. The effect of variation in Π_4 and Π_3 on Π_5 is explored. The model was estimated for 38,400 combinations of parameter values using a MATLAB routine and the results are summarized in Figure 9. The solutions proved to be most sensitive to variation in the dimensionless cleaning cost, Π_4 , and gave different trends depending on the value of Π_4 . The range $0.007 \leq \Pi_4 \leq 800$ was therefore subdivided into four sub-ranges and each is considered in turn below.

Scenario 1: Cheap cleaning, Figure 9 (a): $0.007 \leq \Pi_4 \leq 10$

Figure 9(a) shows that, for a given fouling rate, Π_3 , the optimal time between mechanical cleans (Π_5) is extended as the cost of cleaning increases. This is an expected trend, as the exchanger needs to remain online and recover energy to offset the cost of a process upset associated with a cleaning operation. As the fouling rate increases, the time between cleans decreases, which is also expected. The associated average daily costs are plotted in Figure 9 (a,ii): The reader should note the use of a log scale for Π_5 in Figure 9 (a,i) and a linear scale for Π_6 in Figure 9 (a,ii). The latter shows the anticipated trend, of higher averaged costs with increasing cleaning cost and fouling rate.

Scenario 2: Moderate cleaning cost, Figure 9 (b): $10 \leq \Pi_4 \leq 100$

The same range of fouling rates is considered. The effect of fouling rate on the time between cleans changes as the cost of cleaning increases (increasing Π_4). At lower values ($\Pi_4 \sim 10$), Π_5 decreases with fouling rate, as reported above. At higher values of Π_4 , the optimal operating period decreases and then increases as the fouling rate increases: at intermediate values the optimal operating period is almost insensitive to Π_3 . The change in trends arises because the value of energy recovered while the exchanger is on-line is now small compared to the cleaning cost, so the optimum is now weak. The corresponding overall cost (Figure 9 (b, ii)) indicates that the total daily cost continues to increase, as before. These results demonstrate how the shape of the solution space near the optimal point is sensitive to the model parameters. Similar observations were reported by Pogiatis *et al.* [11].

Scenario 3: Costly cleaning, Figure 9 (c): $100 \leq \Pi_4 \leq 500$

The contour plot of solutions in Figure 9 (c,i) now differs demonstrably from Figure 9 (a,i), both in terms of scale ($400 < \Pi_5 < 10^5$ compared to $10 < \Pi_5 < 200$) and shape. The time between cleans increases with fouling rate and the values of Π_5 indicate that the operating period is much longer than τ_M . Inspection of the Π_6 values in Figure 9 (c, ii) shows that Π_6 quickly approaches 1, which indicates that little energy is being recovered in the exchanger ($\phi_{opt} \sim Q_{cl} C_E$): energy is so cheap (or cleaning so expensive) that the unit spends most of the operating period in the fouled state. Only at lower fouling rates is there any incentive to clean the unit.

Scenario 4: Very expensive cleaning, Figure 9 (d): $500 \leq \Pi_4 \leq 800$

The reader should note that the x- and y- axes in Figure 9 (d) differ from the other plots in order to provide a clearer view of the results. The pattern in scenario (c) is continued, but the timescales are now very large, with $2000 < \Pi_5 < 3 \times 10^6$. Energy is either so cheap or cleaning so costly that the units are not cleaned while the process is operating and the only practical time to clean them is at a shutdown. The use of standby units, to operate while a fouled exchanger is being cleaned, should be considered for such cases.

These results highlight the links between cost, fouling (and exchanger design), and cleaning time. Similar plots can be generated for units with different values of NTU and clean effectiveness (such as different configurations) to establish the regime in which cleaning decisions are likely to lie. Altering NTU is likely to change the clean wall temperature, which is often a key parameter influencing the fouling rate. This can be incorporated by detailed modelling of relationships between Π_1 - Π_4 .

SUPER-CYCLES AND CHOICE OF CLEANING METHODS: AGEING IS RE-INTRODUCED

The dimensional analysis is now applied to the case where ageing occurs and a choice of cleaning methods is available. Foulant deposition subject to ageing is described by the zeroth order two-layer model.

The freshly deposited material adds to the gel layer and this is converted in time to the hard (coke) layer that is not removed by chemical cleaning. Mechanical cleaning removes both gel and coke layers. The deposition and ageing rates are assumed to remain constant over the operating period. The temperature sensitivity discussed earlier (Equation 10) is deemed to be captured approximately in the parameters. The overall fouling rate is given by equation (5), which is written in simple form as

$$\dot{R}_{f,\text{total}} = \dot{R}_{f,c} + \dot{R}_{f,g} \quad (31)$$

Incorporating ageing and choice of cleaning methods introduces 6 additional parameters, namely τ_c , δ_g , δ_c , $C_{cl,c}$, λ_c and λ_g . These lead to the following 4 dimensionless groups.

1. Dimensionless thermal conductivity, Π_7 , given by the ratio of thermal conductivities of gel and coke layers.
2. Dimensionless growth rate, Π_8 , given by the ratio of deposition rates of gel and coke growth rate.
3. Dimensionless cleaning cost, Π_9 , given by the ratio of cleaning costs of chemical and mechanical cleaning.
4. Dimensionless cleaning time, Π_{10} , given by the ratio of cleaning times for a chemical and mechanical clean.

The set of dimensionless groups for the extended problem are summarised in Table 7 along with a likely range of values for the exchanger example described in Table 6.

The super-cycle consists of a series of sub-cycles, the length of each sub-cycle being determined here by a heuristic method. Initially, the cyclically averaged cleaning cost for mechanical cleaning alone, labelled $\Pi_{6,M}$, is evaluated from Equation (30). This serves as a target for comparing the performance of solvent cleaning actions. For a given sub-cycle, Equation (30) is evaluated for solvent cleaning, yielding the cyclically averaged daily cost for solvent cleaning, $\Pi_{6,C}$. The modified formulation is outlined below.

The deposition and ageing rates are assumed to be constant. The overall fouling rate, in dimensionless form is given by

$$\Pi_3 = \dot{R}_{f,\text{total}} U_{cl} \tau_m = (\dot{R}_{f,g} + \dot{R}_{f,c}) U_{cl} \tau_m \quad (32)$$

Differentiating equation (2) with respect to time and substituting into equation (32) gives

$$\Pi_3 = \dot{R}_{f,c} \left(\frac{\delta_g \lambda_c}{\delta_c \lambda_g} + 1 \right) U_{cl} \tau_m \quad (33)$$

In terms of the dimensionless parameters,

$$\Pi_3 = \dot{R}_{f,\text{coke}} \left(\frac{\Pi_8}{\Pi_7} + 1 \right) U_{cl} \tau_m \quad (34)$$

An expression for the rate of coke formation is thus given by

$$\dot{R}_{f,c} = \frac{\Pi_3}{\left(\frac{\Pi_8}{\Pi_7} + 1\right) U_{cl} \tau_M} \quad (35)$$

If chemical cleaning is performed after time t , this will not remove the coke layer and the overall heat transfer coefficient after cleaning (compared to the completely clean state) is given by

$$\frac{1}{U} = \frac{1}{U_{cl}} + \dot{R}_{f,c} t \quad (36)$$

NTU after a chemical cleaning, Π_1^* , is given by

$$\Pi_1^* = \frac{UA}{W_{\min}} = \frac{U_{cl} A}{W_{\min} \left(\frac{1}{1 + U_{cl} \dot{R}_{f,c} \tau_c \left(\frac{t}{\tau_c} \right)} \right)} \quad (37)$$

Substituting (35) into (37) and using dimensionless groups in Tables 6 and 7 gives

$$\Pi_1^* = \Pi_1 \left(\frac{1}{1 + \frac{\Pi_3}{\left(\frac{\Pi_8}{\Pi_7} + 1\right)} \Pi_{10} \Pi_5^*} \right) \quad (38)$$

The optimum cleaning cycle for a chemical cleaning action after a chemical cleaning, $\Pi_{5,c}$, can now be written based on equation (28) as

$$(\Pi_{5,c} + 1) \left(1 - \frac{\frac{1}{\Pi_2^*}}{\frac{1}{\Pi_1^*} + 1 + \frac{\Pi_3 \Pi_{5,c}}{\Pi_1^*}} \right) = \left(\Pi_{5,c} - \frac{\Pi_1^*}{\Pi_2^* \Pi_3} \ln \left| \frac{1 + \Pi_1^* + \Pi_3 \Pi_{5,c}}{1 + \Pi_1^*} \right| + 1 + \Pi_4^* \right) \quad (39)$$

Here, $\Pi_{5,c} = \frac{\Pi_5}{\Pi_{10}}$; $\Pi_4^* = \frac{\Pi_4 \Pi_9}{\Pi_{10}}$; $\Pi_2^* = \frac{\Pi_1^*}{\Pi_1^* + 1}$ and $\Pi_3^* = \Pi_3 \Pi_{10}$

Based on equation (30), the cyclically averaged daily cost for the chemical cleaning cycle is given by

$$\Pi_{6,c} = \frac{\left[\Pi_{5,c} - \frac{\Pi_1^*}{\Pi_2^* \Pi_3} \ln \left| \frac{1 + \Pi_1^* + \Pi_3 \Pi_{5,c}}{1 + \Pi_1^*} \right| + 1 \right] + \Pi_4^*}{(\Pi_{5,c} + 1)}$$

When $\Pi_{6,c} < \Pi_{6,M}$, solvent cleaning is preferred. At the end of the cleaning operation δ_g is set to zero and the calculation is repeated for the next sub-cycle. Otherwise, mechanical cleaning is the preferred option. The time t is also reset to zero. After a number of solvent cleans, mechanical cleaning will be preferred and the problem is then restarted. The period between the time when the exchanger starts operating at its initial, clean condition to the end of the sub-cycle ending with a mechanical clean is defined as the length of the 'cleaning super-cycle'.

If there are $n+1$ sub-cycles in each super-cycle, the length of the super-cycle is given by

$$\text{Super cycle} = \sum_{i=1}^n (t_{opt,i} + \tau_c) + (t_{opt,m} + \tau_m)$$

$$\frac{\text{Super cycle}}{\tau_m} = \sum_{i=1}^n \left(\frac{t_{opt,i} \tau_c}{\tau_c \tau_m} + \frac{\tau_c}{\tau_m} \right) + \left(\frac{t_{opt,m}}{\tau_m} + 1 \right) \quad (40)$$

or in dimensionless form,

$$\frac{\text{Super cycle}}{\tau_m} = \sum_{i=1}^n \Pi_{10} (\Pi_{5,i} + 1) + (\Pi_{5,M} + 1) \quad (41)$$

The average total cost incurred due to fouling over a super-cycle is then

$$\text{Minimum daily average of a super cycle} = \frac{\sum_{i=1}^n \phi_{i,c} (t_{opt,i} + \tau_c) + \phi_M (t_{opt} + \tau_m)}{\sum_{i=1}^n (t_{opt,i} + \tau_c) + (t_{opt} + \tau_m)} \quad (42)$$

Or, in dimensionless form

$$\frac{\text{Minimum daily average of a super cycle}}{C_E Q_{cl}} = \frac{\sum_{i=1}^n \frac{\phi_{i,c}}{C_E Q_{cl}} \Pi_{10} (\Pi_{5,i} + 1) + \frac{\phi_M}{C_E Q_{cl}} (\Pi_{5,M} + 1)}{\sum_{i=1}^n \Pi_{10} (\Pi_{5,i} + 1) + (\Pi_{5,M} + 1)} \quad (43)$$

Illustration

The exchanger of Figure 9 is subject to ageing described by the two-layer ageing model. The dimensionless parameters were selected as $\Pi_7 = 0.2$, $\Pi_8 = 0.1$, $\Pi_9 = 0.1$ and $\Pi_{10} = 0.1$, giving a clean initial effectiveness of 0.9 (i.e. $\Pi_2 = 0.9$, hence $\Pi_1 = 9$). The effect on Π_5 of variation of Π_4 and Π_3 is explored. The Π_4 values were varied from 0 to 10.

Figure 10(a) shows that the length of the super-cycle increases as mechanical cleaning becomes more costly (or energy cheap, increasing Π_4). The number of solvent cleaning actions in each optimised super-cycle is marked on Figure 10 (a). As a discrete action, solvent cleaning gives rise to a series of steps in the solution plane. Each of the steps presents a non-linear surface. The surfaces exhibit the behaviour discussed in Figure 9 (a, b), where the time for a super-cycle increases with increased cost of mechanical cleaning and decreases with increasing rate of deposition. The Figure shows that more chemical cleans are employed as mechanical cleaning becomes less attractive. The super-cycle time is not very sensitive to fouling rate (Π_3) for the parameters considered, until large values of Π_4 . Figure 10(b) presents the corresponding minimum daily average cost for a super-cycle (calculated through equation 43), and here the value is quite sensitive to the fouling rate.

Whereas Figure 10 shows the overall landscape, Figure 11 provides a comparison of two cleaning scenarios for an exchanger which give Π_4 values at either end of the range, namely

- (i) 'Reactive cleaning', where energy and production costs are high, at 10 k\$/day.
- (ii) 'Pro-active cleaning', where energy and production costs are modest, at 1 k\$/day.

The mechanical cleaning cost is set at 20 000 \$ and takes 3 days, whereas chemical cleaning takes 1 day at a cost of 2000 \$. This gives $\Pi_9 = 0.1$ (as in Figure 10) and $\Pi_{10} = \tau_c / \tau_m = 0.333$. For a 2 MW exchanger with a U_{cl} of $800 \text{ W m}^{-2} \text{ K}^{-1}$, setting $C_E Q_{cl} = 10000 \text{ $/day}$ gives $\Pi_4 = 0.67$ for the reactive cleaning scenario, while in the pro-

active scenario $\mathcal{I}_4 = 6.67$. Figure 11 compares the optimal solutions for the range of (dimensionless) fouling rates, $0.01 < \mathcal{I}_3 < 0.02$, corresponding to absolute fouling rates of 4.8×10^{-11} to $9.6 \times 10^{-11} \text{ m}^2\text{K J}^{-1}$. Table 8 summarises the dimensional parameters for these calculations.

Figure 11(a) shows that the super-cycle duration decreases in both scenarios as the fouling rate increases, which is accompanied by an increase in the average daily cost (Figure 11(b)). The length of the super-cycle is noticeably different for the two scenarios, differing by a factor of about 3 \times , from 35-50 $\times \tau_m$ (105-150 days) for reactive cleaning to 110-135 $\times \tau_m$ (330-405 days) for the proactive scenario. In this example, the proactive cleaning schedule includes two chemical cleaning actions before a mechanical cleaning, whereas the reactive cleaning schedule includes only a single mechanical cleaning. Less (or no) chemical cleaning actions are expected for a reactive cleaning schedule as the energy penalty is high when the exchanger is offline for cleaning.

The dimensionless average daily costs vary from 0.12-0.17 for reactive cleaning to 0.27-0.37 for pro-active cleaning, but the ten-fold difference in cleaning costs more counters this difference, to give average daily costs of 270-370 \$ day⁻¹ (for proactive cleaning) and 1200-1700 \$ day⁻¹ (reactive cleaning). As before, higher fouling rates require more regular cleaning and incur higher overall costs. These values depend of the ageing parameters (\mathcal{I}_7 and \mathcal{I}_8), but this is not explored further here.

This analysis identifies combinations of parameters which will favour mechanical or mixed cleaning strategies for mitigating fouling. The fouling and ageing rates used as inputs to the analysis will, however, be influenced by the choice of exchanger type and configuration as the design choices determine the temperature and flow field in the unit. The framework now exists for closing the design-fouling-cleaning loop, in that once a candidate exchanger design is identified (setting the capital cost), the optimal operating cost can be estimated (setting energy and cleaning costs) and the total amortised cost of that design estimated, for comparison with others. Detailed calculations can then be performed on selected candidates.

CONCLUSIONS

The first order ageing model was used to link heat transfer and cleaning effectiveness in a case study involving optimisation of the cleaning schedule where there is a choice between two different cleaning methods. The resultant mixed cleaning strategy gives rise to a cleaning super-cycle, with the number of chemical cleaning actions dictated by several factors, including the relative time and cost of the two cleaning methods.

A generalized super-cycle is presented which highlights the key parameters, or combination of parameters, determining the optimal cleaning cycle. The general formulation offers a systematic approach to assessing cleaning-based strategies for mitigating fouling, as the scope for improving process operating time and profitability can be estimated.

The effect of ageing on the performance of simple heat exchangers has been considered. Different models for describing the thermal effects of deposit ageing are presented and compared. The first order, two layer model proved to be quite robust in mimicking the distributed ageing model presented by Ishiyama *et al.* (2010), suggesting that this mathematical form should be used to describe experimental data and/or used in simulations.

ACKNOWLEDGEMENTS

Discussions with Thomas Pogiatzis and Vassilis Vassiliadis are gratefully acknowledged, as are helpful suggestions from the reviewers. This paper draws together several strands of work on fouling in our group that were inspired by papers published by Professor Müller-Steinhagen and his co-workers as well as the conferences he has led and co-organised.

MATLAB code

The authors are happy to provide interested readers with the Matlab® code used to generate the results in Figures 9 and 10. Please contact Dr Edward Ishiyama at ishiyama.edward@gmail.com.

NOMENCLATURE

Roman

A	surface area, m^2
a_1	parameter in Eqn. 15, $J m^{-2} K^{-1}$
a_2	parameter in Eqn. 15, s
a_3	parameter in Eqn. 20, J
a_4	parameter in Eqn. 20, s
a_0	pre-exponential term in Eqn. 8, $m s^{-1}$
a_I	pre-exponential term in Eqn. 9, s^{-1}
a_{II}	pre-exponential term of Model II, s^{-1}
a_d	pre-exponential term in Eqn. 6, $m^2 K J^{-1}$
C_E	energy cost, US \$ $W^{-1} day^{-1}$
C_{cl}	cost of a cleaning action, US\$ $clean^{-1}$
DT	stream temperature change, K
E_d	activation energy for deposition, $J mol^{-1}$
E_0	activation energy in Eqn. 8, $kJ mol^{-1}$
E_I	activation energy in Eqn. 9, $kJ mol^{-1}$
E_{II}	activation energy of Model II, $kJ mol^{-1}$
k_0	kinetic parameter, zeroth order ageing, $m s^{-1}$
k_I	kinetic parameter, first order ageing, s^{-1}
N_C	number of chemical cleaning actions, -
Pr	Prandtl number, -
Q	heat duty, W
R	gas constant, $J mol^{-1} K^{-1}$
Re	Reynolds number, -
r_c	rate of coke formation, $m s^{-1}$
r_d	net rate of deposition, $m s^{-1}$
R_f	fouling resistance, $m^2 K W^{-1}$
\dot{R}_f	fouling rate, $m^2 K J^{-1}$
t	time, days
t^*	relative time in Figures 3 and 4, -
t_C	time at a chemical clean, days
t_M	time at a mechanical clean, days
T	temperature, K
TAL	total averaged loss, US \$ day^{-1}
U	overall heat transfer coefficient, $W m^{-2} K^{-1}$
W	heat capacity flow rate, $J s^{-1} K^{-1}$
x	linear co-ordinate, m

Greek

α, β	parameters in property prediction equations, Table 4
δ	deposit thickness, m
$\dot{\delta}$	deposit growth rates, m s^{-1}
ε	effectiveness, -
ϕ	cyclically averaged operational cost, $\text{US \$ day}^{-1}$
λ	deposit thermal conductivity, $\text{W m}^{-1} \text{K}^{-1}$
Π_1	clean NTU, -
Π_2	clean effectiveness, -
Π_3	dimensionless fouling rate, -
Π_4	dimensionless cost, -
Π_5	dimensionless optimal cycle time, -
Π_6	dimensionless average minimum operating cost, -
Π_7	dimensionless thermal conductivity, -
Π_8	dimensionless deposition rate, -
Π_9	dimensionless cleaning cost, -
Π_{10}	dimensionless cleaning time, -
τ	time taken for a cleaning action, days

Subscripts

c	coke layer
C	chemical
cl	clean
cold	cold stream
g	gel layer
hot	hot stream
i	index for pre-exponential term in Eqn. 10/ index for sub-cycle in Eqns. 40-43
int	interface between gel and coke
j	index for activation energy in Eqn. 10
M	mechanical
max	maximum
min	minimum
opt	optimal condition
s	surface

Acronym

NTU	number of transfer units
-----	--------------------------

REFERENCES

- [1] Ma, R.S.T., and Epstein, N., Optimum cycles for falling rate processes, *Canadian Journal of Chemical Engineering*, vol. 59, pp. 631–633, 1981.
- [2] Casado, E., Model optimizes exchanger cleaning, *Hydrocarbon Processing*, vol. 69, pp. 71–76, 1990.
- [3] Sheikh, A.K., Zubair, S.M., Haq, M.U., and Budair, M.O., Reliability-based maintenance strategies for heat exchangers subject to fouling, *Journal of Energy Resources Technology, Transactions of the ASME*, 118, pp. 306–312, 1996.
- [4] Müller-Steinhagen, H., and Branch, C.A. Heat transfer and heat transfer fouling in Kraft black liquor evaporators, *Experimental Thermal and Fluid Science*, vol. 14, pp. 425–r37, 1997.
- [5] Georgiadis, M.C. and Papageorgiou, L.G. Optimal energy and cleaning management in heat exchanger networks under fouling, *Chemical Engineering Research and Design*, vol. 78, pp. 168–179, 2000.
- [6] Ishiyama, E.M., Paterson, W.R. and Wilson, D.I., Platform for techno-economic analysis of fouling mitigation options in refinery preheat trains, *Energy and Fuels*, vol. 23, pp. 1323–1337, 2009.
- [7] Ishiyama, E.M., Heins, A.V., Paterson, W.R., Spinelli, L., and Wilson, D.I., Scheduling cleaning in a crude oil preheat train subject to fouling: Incorporating desalter control, *Applied Thermal Engineering*, vol. 30, pp. 1852–1862, 2010.
- [8] Müller-Steinhagen, H., *Heat Exchanger Fouling - Mitigation and Cleaning Technologies*, UK: IChemE, 2000.
- [9] Wilson, D.I., Challenges in cleaning: Recent developments and future prospects, *Heat Transfer Engineering*, vol. 26, pp. 51–59, 2005.
- [10] Ishiyama, E.M., Paterson, W.R., and Wilson, D.I., Optimum cleaning cycles for heat transfer equipments undergoing fouling and ageing, *Chemical Engineering Science*, vol. 66:4, pp. 604-612, 2010.
- [11] Pogiatzis, T., Ishiyama, E.M., Paterson, W.R., Vassiliadis, V.S., and Wilson, D.I., Identifying optimal cleaning cycles for heat exchangers subject to fouling and ageing, *Applied Energy*, vol. 89, pp. 60–66, 2012.
- [12] Crittenden, B.D. and Kolaczkowski, S.T. Energy savings through the accurate prediction of heat transfer fouling resistances. *Energy for Industry*, London: Pergamon Press, pp. 257–266, 1979.
- [13] Fan, Z., and Watkinson, A.P., Formation and characteristics of carbonaceous deposits from heavy hydrocarbon coking vapors, *Industrial and Engineering Chemistry Research*, vol. 45, pp. 6428–6435, 2006.
- [14] Ishiyama, E.M., Coletti, F., Macchietto, S., Paterson, W.R., and Wilson, D.I., Impact of deposit ageing on thermal fouling: Lumped parameter model, *AIChE Journal*, vol. 56, pp. 531–545, 2010.
- [15] Ishiyama, E.M., Paterson, W.R., and Wilson, D.I., Exploration of alternative models for the aging of fouling deposits, *AIChE Journal*, vol. 57, pp. 3199–209, 2011.
- [16] Yeap, B.L., Wilson, D.I., Polley, G.T., and Pugh, S.J., Mitigation of crude oil refinery heat exchanger fouling through retrofits based on thermo-hydraulic fouling models., *Chemical Engineering Research and Design*, vol. 82, pp. 53–71, 2004.
- [17] Derakhshesh, M., Eaton, P., Newman, B., Hoff, A., Mitlin, D., and Gray, M.R., Effect of asphaltene stability on fouling at delayed coking process furnace conditions, *Energy and Fuels*, 2013, DOI: 10.1021/ef301754y

- [18] Ishiyama, E.M., Paterson, W.R., and Wilson, D.I., Thermo-hydraulic channelling in parallel heat exchangers subject to fouling, *Chemical Engineering Science*, vol. 63, pp. 3400–3410, 2008.
- [19] Coletti, F., Ishiyama, E.M., Paterson, W.R., Wilson, D.I., and Macchietto, S., Impact of deposit aging and surface roughness on thermal fouling: Distributed model, *AIChE Journal*, vol. 56, pp. 3257–3273, 2010.

Table 1: Kinetic parameters used in exploring ageing kinetics [10].

Model	Ageing	$E_0 = E_I = E_{II} / \text{kJ mol}^{-1}$		
		10	50	200
Model 0 a_0 (m day ⁻¹)	Slow	3.5×10^{-6}	0.1	0.20×10^{13}
	Medium	6.0×10^{-6}	1.0	0.85×10^{13}
	Fast	6.4×10^{-6}	10	1.2×10^{13}
Model I a_I (day ⁻¹)	Slow	0.06	0.1	5.6×10^{16}
	Medium	0.40	1.0	7.0×10^{17}
	Fast	0.85	10	3.4×10^{18}
Model II a_{II} (day ⁻¹)	Slow	0.024	0.1	4.5×10^{16}
	Medium	0.24	1.0	4.5×10^{17}
	Fast	2.40	10	4.5×10^{18}

Table 2: Summary of relative agreement of the two-layer models with Model II for constant heat flux operation.
Entry indicates good agreement

Activation energy	<i>Ageing rate</i>		
	Slow	Medium	Fast
$E_i = 10 \text{ kJ mol}^{-1}$	Model I	Model I	Both
$E_i = 50 \text{ kJ mol}^{-1}$	Model I	Model I	Both
$E_i = 200 \text{ kJ mol}^{-1}$	Both	Both	Both

Table 3: Summary of relative agreement of the two-layer models with Model II for constant wall temperature operation. Entry indicates good agreement

Activation energy	<i>Ageing rate</i>		
	Slow	Medium	Fast
$E_i = 10 \text{ kJ mol}^{-1}$	Model I	Model I	Both
$E_i = 50 \text{ kJ mol}^{-1}$	Model I	Neither	Both
$E_i = 200 \text{ kJ mol}^{-1}$	Neither	Neither	Neither

Table 4: Case study stream properties [T in °C]

Cold stream	
Density, kg m^{-3}	$882.1 - 0.801 T$
Dynamic viscosity, Pa s	$\alpha \exp(\beta/T (T + 273.15)); \alpha = 0.32 \times 10^{-5}; \beta = 2396.3$
Specific heat capacity, $\text{J kg}^{-1} \text{K}^{-1}$	$1890 + 3.805 T$
Thermal conductivity, $\text{W m}^{-1} \text{K}^{-1}$	$0.129 - 0.0013 T$
Hot stream	
Density, kg m^{-3}	$934.3 - 0.720 T$
Dynamic viscosity, Pa s	$\alpha \exp(\beta/T (T + 273.15)); \alpha = 2.145 \times 10^{-14}; \beta = 11735$
Specific heat capacity, $\text{J kg}^{-1} \text{K}^{-1}$	$1893 + 3.540 T$
Thermal conductivity, $\text{W m}^{-1} \text{K}^{-1}$	$0.129 - 0.0013 T$

Table 5: Case study exchanger specifications

Description	Value
Tube length	6 m
Tube external diameter	0.0254 m
Tube internal diameter	0.0199 m
Total number of tubes	800
No. of tube side passes	1
Shell diameter	1.3 m
Baffle spacing	0.3 m
Baffle cut	25 %
Initial fouling resistance	$0 \text{ m}^2\text{K W}^{-1}$
Clean overall heat transfer coefficient	$900 \text{ W m}^{-2}\text{K}^{-1}$
Cold stream flow/inlet temperature	$256 \text{ kg s}^{-1} / 220 \text{ }^\circ\text{C}$
Hot stream flow/inlet temperature	$60 \text{ kg s}^{-1} / 320 \text{ }^\circ\text{C}$

Table 6: Dimensionless group for mechanical cleaning cycle

Dimensionless group		Typical industrial values	Range
Clean NTU (Π_1)	$\frac{U_{cl}A}{C_{min}\Delta T_{max}}$		$0.1 < \Pi_1 < 10$
Clean effectiveness (Π_2)	$\frac{Q_{cl}}{C_{min}\Delta T_{max}}$		$0 < \Pi_2 < 1$
Dimensionless fouling rate (Π_3)	$\dot{R}_f U_{cl} \tau_M$	$0 < \dot{R}_f < 1 \times 10^{-10}$ (m ² K J ⁻¹) $0 < \tau_M < 14$ (days) $50 < U_{cl} < 1000$ (W m ⁻² K ⁻¹)	$0 < \Pi_3 < 0.12$
Dimensionless cost (Π_4)	$\frac{C_{cl,M}}{\tau_M Q_{cl} C_E}$	$2000 < C_{cl,M} < 40,000$ (US\$ clean ⁻¹) $1 < \tau_M < 14$ (days) $0 < Q_{cl} < 10$ (MW) $0.5 < C_E < 2$ (US\$ kW ⁻¹ day ⁻¹)	$0.007 < \Pi_4 < 800$
Dimensionless time (Π_5)	$\frac{t_{opt}}{\tau_M}$	Objective function	
Dimensionless minimum daily averaged cost (Π_6)	$\frac{\phi_{min}}{C_E Q_{cl}}$	ϕ_{min} is the minimum daily averaged cost (i.e. at t_{opt}). This value can never be greater than $C_E Q_{cl}$ as Q_{cl} is the maximum amount of energy lost per unit time.	

Table 7: Additional dimensionless group for cleaning super-cycle

Dimensionless group		Range – comments*	Value
Π_7	Ratio of gel thermal conductivity to that of coke $\frac{\lambda_g}{\lambda_c}$	For a crude refinery application the thermal conductivities of soft gels and hard cokes lie between 0.1 – 0.2 and 1 - 2 W m ⁻¹ K ⁻¹ , respectively.	$0.05 < \Pi_7 < 0.2$
Π_8	Rate of gel deposition over the rate of coke formation $\frac{\dot{\delta}_g}{\dot{\delta}_c}$	The rate of coke formation is always less than or equal to the rate of gel formation as the formation of gel provides a limiting step.	$0 < \Pi_8 < 1$
Π_9	Cost of chemical cleaning over cost of mechanical cleaning $\frac{C_{cl,C}}{C_{cl,M}}$	The cost of mechanical cleaning could be 10 times more than chemical cleaning.	$0.1 < \Pi_9 < 1$
Π_{10}	Ratio of time taken for chemical cleaning to that for mechanical cleaning $\frac{\tau_{cl,C}}{\tau_{cl,M}}$	Time taken for mechanical cleaning could be 1–10× longer than chemical cleaning.	$0.1 < \Pi_{10} < 1$

* based on data for practical crude refinery operation and heat exchangers in refinery service

Table 8: Summary of dimensional and dimensionless parameters for exchanger in Figure 11

Parameter	Value
U_{cl}	800 W m ⁻² K ⁻¹
Q_{cl}	2 MW
τ_M	3 days
τ_C	1 day
$C_{cl,M}$	20000 US\$ per clean
$C_{cl,C}$	2000 US\$ per clean
C_E	10000 US\$ per day (reactive cleaning) 1000 US\$ per day (proactive cleaning)
\dot{R}_f	4.8×10^{-11} m ² K J ⁻¹
λ_g	0.1 W m ⁻¹ K ⁻¹

List of Figure Captions

- Figure 1: Fouling-cleaning cycle showing impact of chemical and mechanical cleaning (based on Wilson [9])
- Figure 2: Schematic comparison of (a) distributed and (b) two-layer ageing models. The deposit changes from its initial gel form to a harder, coke, form over time. Darkness of shading indicates extent of ageing.
- Figure 3: Comparison of ageing models under constant heat flux operation. Key in (a) common to all plots. t^* is a relative time scale where $t^* = 1$ indicates that the time taken for the tube-side heat transfer coefficient to decrease to 50% of its initial value at the initial fouling rate. *Reproduced from [15], © John Wiley & Sons.*
- Figure 4: Comparison of ageing models under constant wall temperature operation. Key in (a) common to all plots. t^* is a relative time scale where $t^* = 1$ indicates that the time taken for the tube-side heat transfer coefficient to decrease to 50% of its initial value at the initial fouling rate. *Reproduced from [15], © John Wiley & Sons.*
- Figure 5: Schematic of the impact of ageing described by the two-layer model on (a) deposition, and (b) heat transfer. I - deposit, thickness δ , grows and an aged layer, labelled 'coke', grows simultaneously; II - solvent cleaning at time t_c leaves the aged layer – deposition restarts from δ_c ; III - mechanical cleaning at time t_m removes all deposit and deposition restarts from a clean surface. τ_m is the duration of the mechanical cleaning step; the duration of the chemical cleaning step, τ_c , is zero here.
- Figure 6: Effect of ageing on (a) overall fouling resistance and (b) deposit thickness after 1000 days of operation.
- Figure 7: Evolution of (a) overall fouling resistance and (b) local value of average daily cost. Labels C and M denote chemical and mechanical cleaning actions, respectively. Periods I and II represent sub-cycles ending with a chemical clean; period III ends with mechanical cleaning. Parameters: $C_{c,M}/C_{c,C} = 1.5$, $\tau_m/\tau_c = 7$, $a_1 = 500 \text{ day}^{-1}$.
- Figure 8: Effect of cost ratio and cleaning duration ratio on (a) super-cycle period and (b) total averaged daily cost for $a_1 = 500 \text{ day}^{-1}$. Symbols indicate a mixed cleaning scenario: numerical values indicate the number of chemical cleaning actions per super-cycle. The surface in (b) shows the cost for mechanical cleaning alone
- Figure 9: Variation of (i) II_5 (note log scale) and (ii) II_6 with II_3 and II_4 : (a – d) denote different ranges of cleaning cost, II_4 . Arrows indicate scale direction.
- Figure 10: Variation in dimensionless (a) super-cycle time and (b) cost under a range of fouling rates (II_3) and mechanical cleaning cost (II_4).

Figures

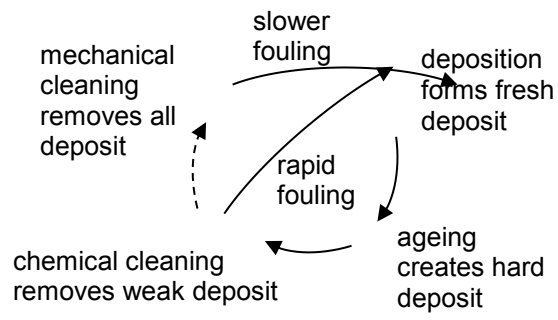


Figure 1: Fouling-cleaning cycle showing impact of chemical and mechanical cleaning (based on Wilson [9])

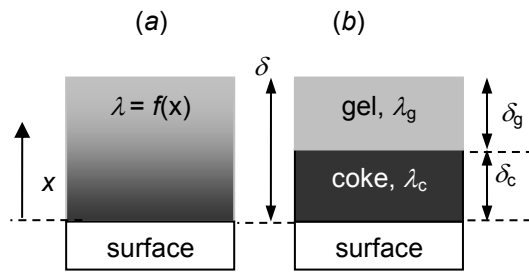
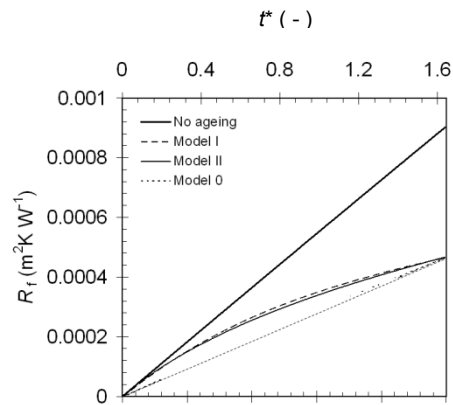
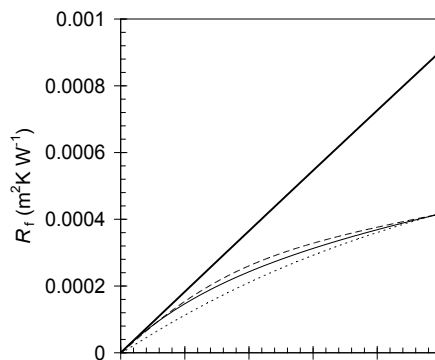


Figure 2: Schematic comparison of (a) distributed and (b) two-layer ageing models. The deposit changes from its initial gel form to a harder, coke, form over time. Darkness of shading indicates extent of ageing.

(a) $E_0 = E_I = E_{II} = 10 \text{ kJ mol}^{-1}$



(b) $E_0 = E_I = E_{II} = 50 \text{ kJ mol}^{-1}$



(c) $E_0 = E_I = E_{II} = 200 \text{ kJ mol}^{-1}$

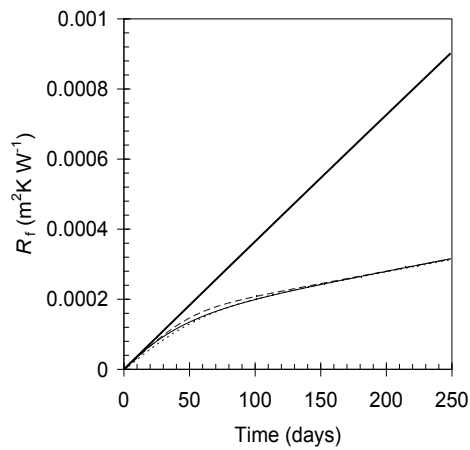
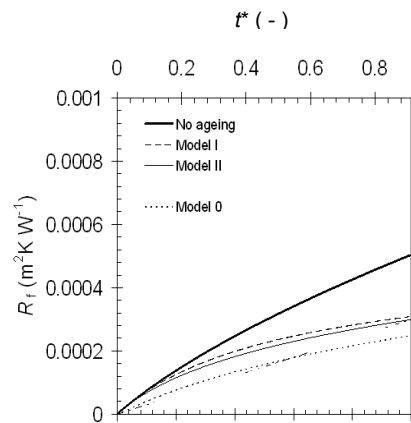
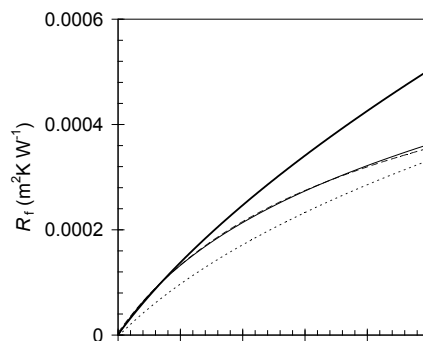


Figure 3: Comparison of ageing models under constant heat flux operation. Key in (a) common to all plots. t^* is a relative time scale where $t^* = 1$ indicates that the time taken for the tube-side heat transfer coefficient to decrease to 50% of its initial value at the initial fouling rate. *Reproduced from [15], © John Wiley & Sons.*

(a) $E_0 = E_I = E_{II} = 10 \text{ kJ mol}^{-1}$



(b) $E_0 = E_I = E_{II} = 50 \text{ kJ mol}^{-1}$



(c) $E_0 = E_I = E_{II} = 200 \text{ kJ mol}^{-1}$

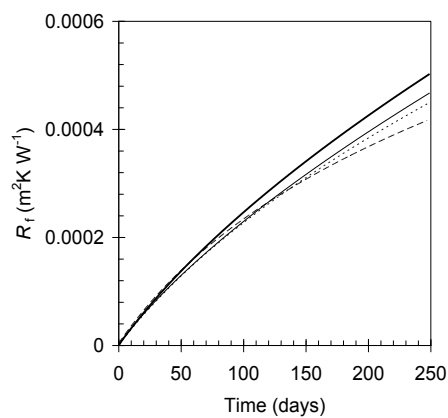


Figure 4: Comparison of ageing models under constant wall temperature operation. Key in (a) common to all plots. t^* is a relative time scale where $t^* = 1$ indicates that the time taken for the tube-side heat transfer coefficient to decrease to 50% of its initial value at the initial fouling rate. *Reproduced from [15], © John Wiley & Sons.*

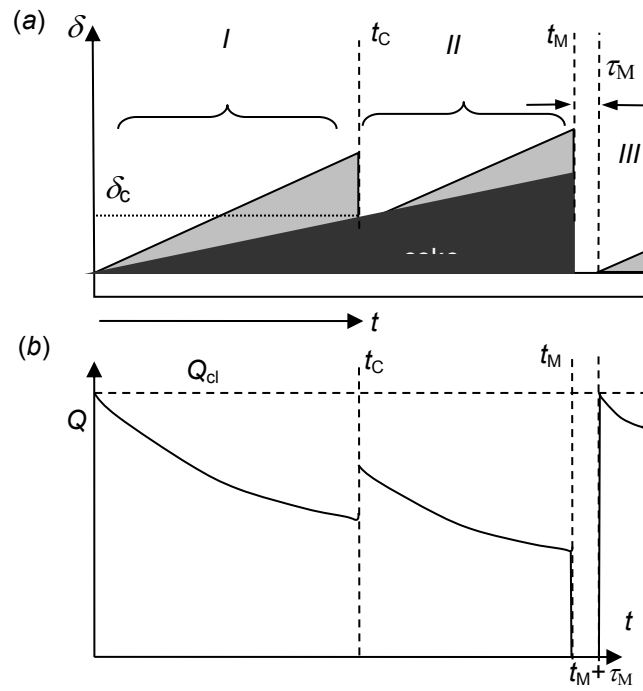
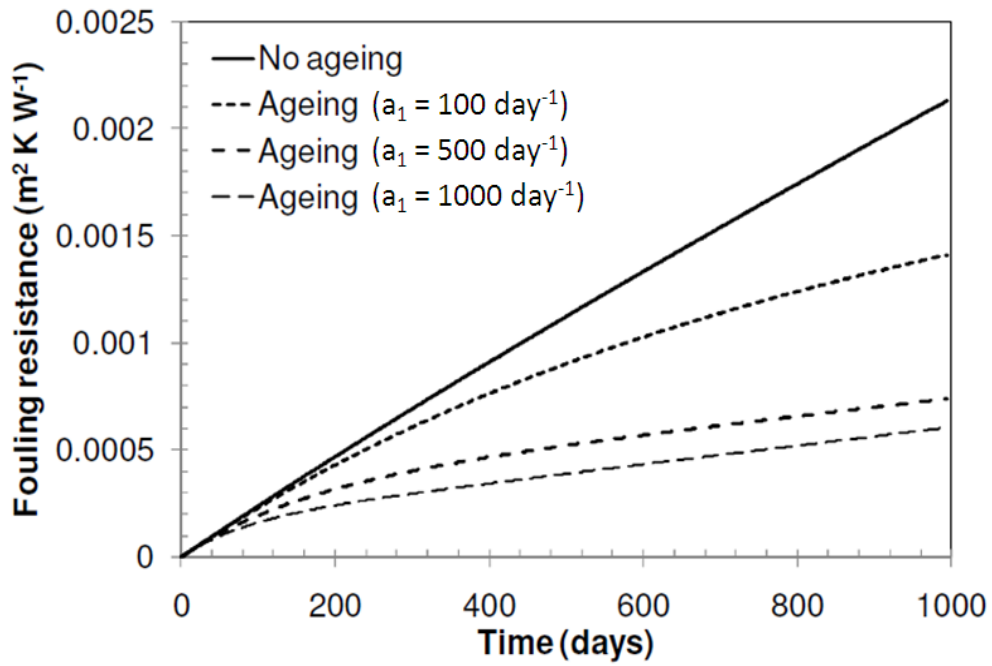


Figure 5: Schematic of the impact of ageing described by the two-layer model on (a) deposition, and (b) heat transfer. I - deposit, thickness δ , grows and an aged layer, labelled 'coke', grows simultaneously; II - solvent cleaning at time t_c leaves the aged layer – deposition restarts from δ_c ; III - mechanical cleaning at time t_M removes all deposit and deposition restarts from a clean surface. τ_M is the duration of the mechanical cleaning step; the duration of the chemical cleaning step, τ_c , is zero here.

(a)



(b)

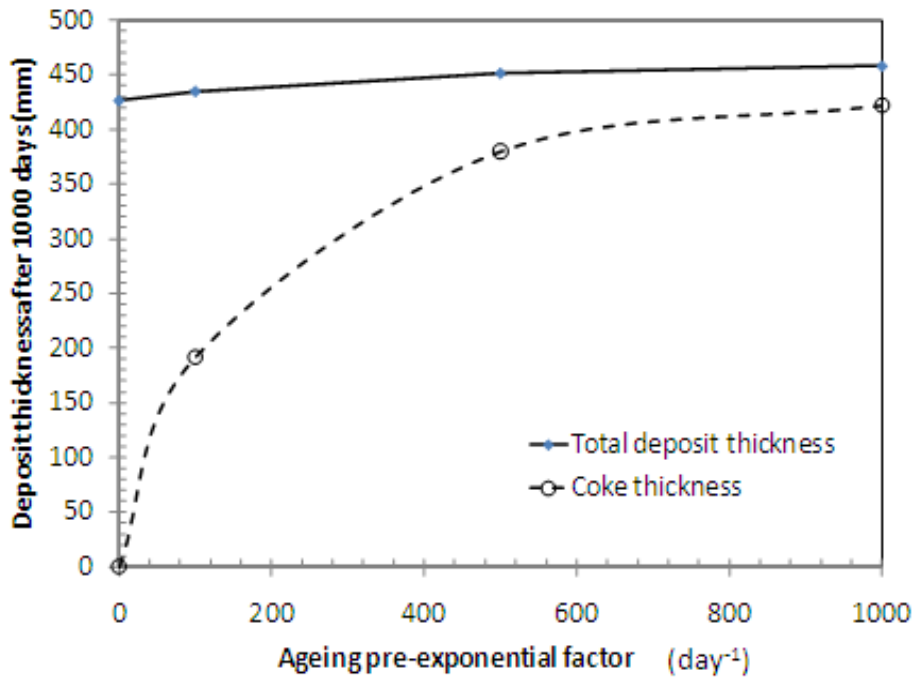


Figure 6: Effect of ageing on (a) overall fouling resistance and (b) deposit thickness after 1000 days of operation.

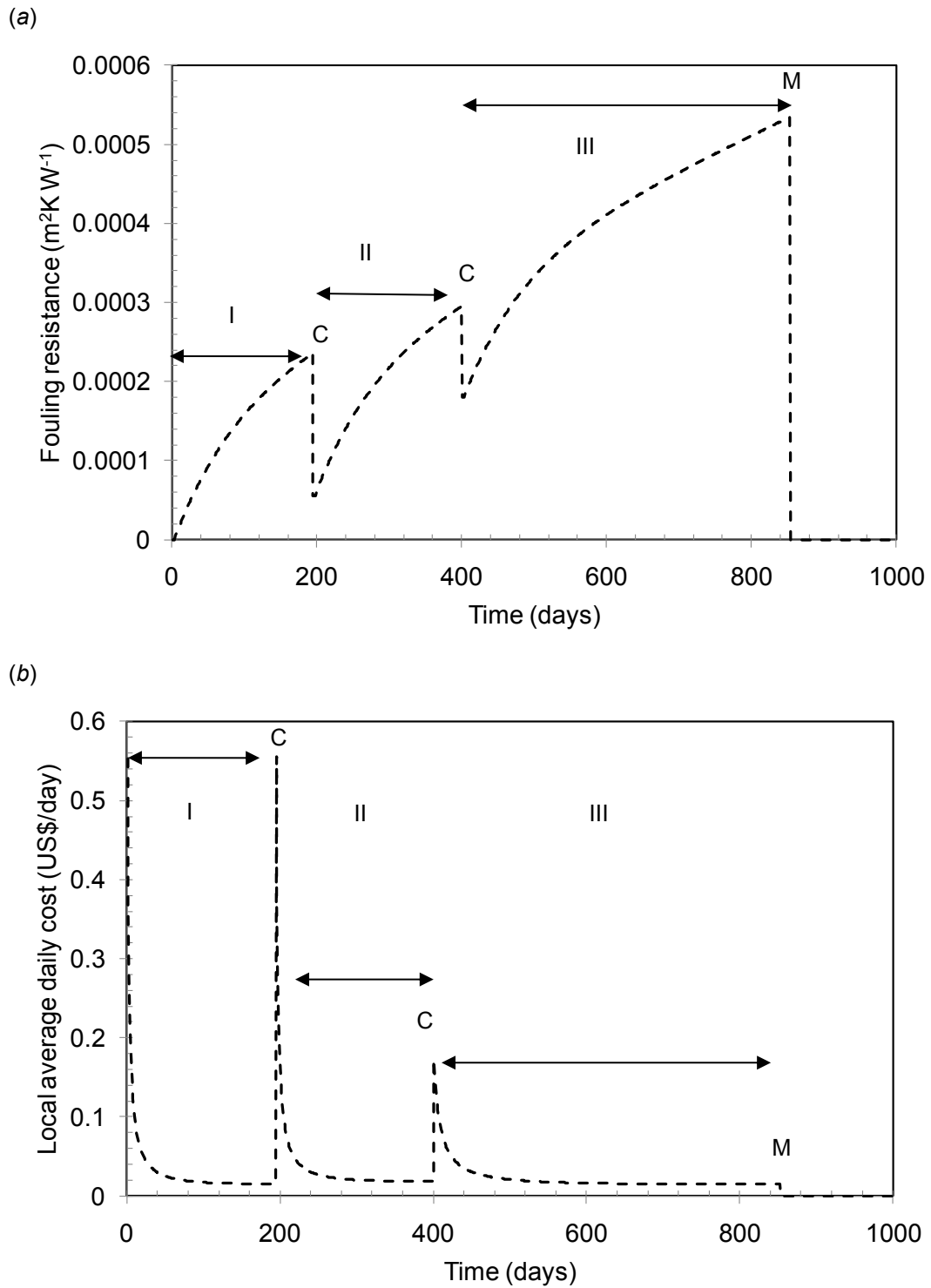
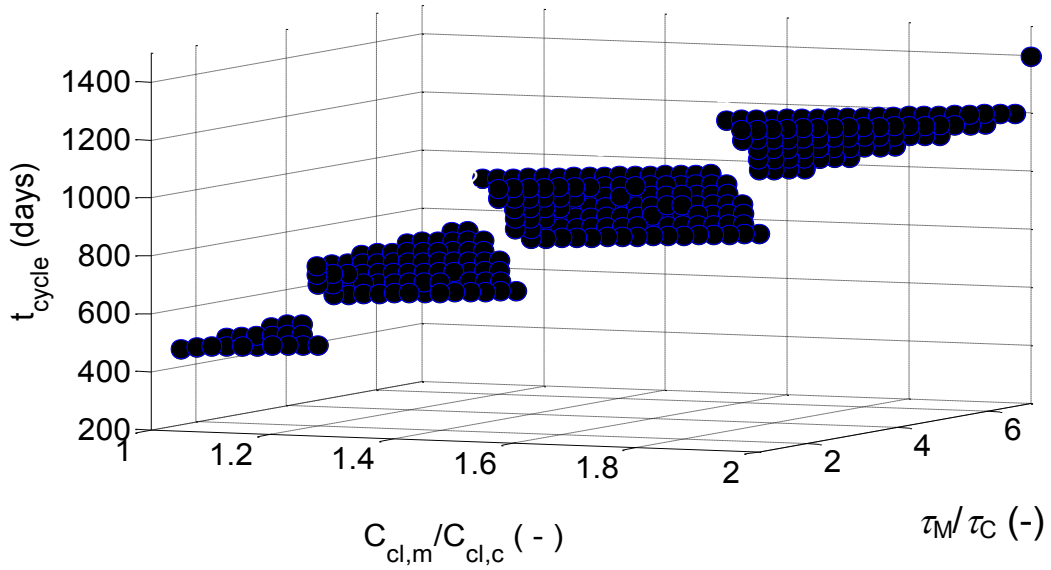


Figure 7: Evolution of (a) overall fouling resistance and (b) local value of average daily cost. Labels C and M denote chemical and mechanical cleaning actions, respectively. Periods I and II represent sub-cycles ending with a chemical clean; period III ends with mechanical cleaning. Parameters: $C_{c,M}/C_{c,C} = 1.5$, $\tau_M/\tau_C = 7$, $a_1 = 500 \text{ day}^{-1}$.

(a)



(b)

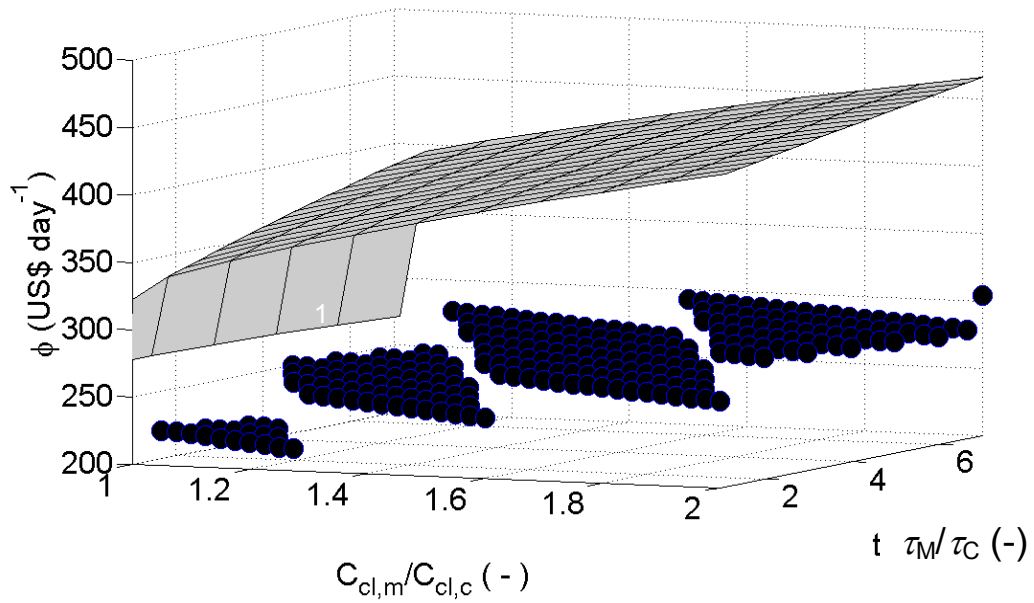


Figure 8: Effect of cost ratio and cleaning duration ratio on (a) super-cycle period and (b) total averaged daily cost for $a_1 = 500 \text{ day}^{-1}$. Symbols indicate a mixed cleaning scenario: numerical values indicate the number of chemical cleaning actions per super-cycle. The surface in (b) shows the cost for mechanical cleaning alone

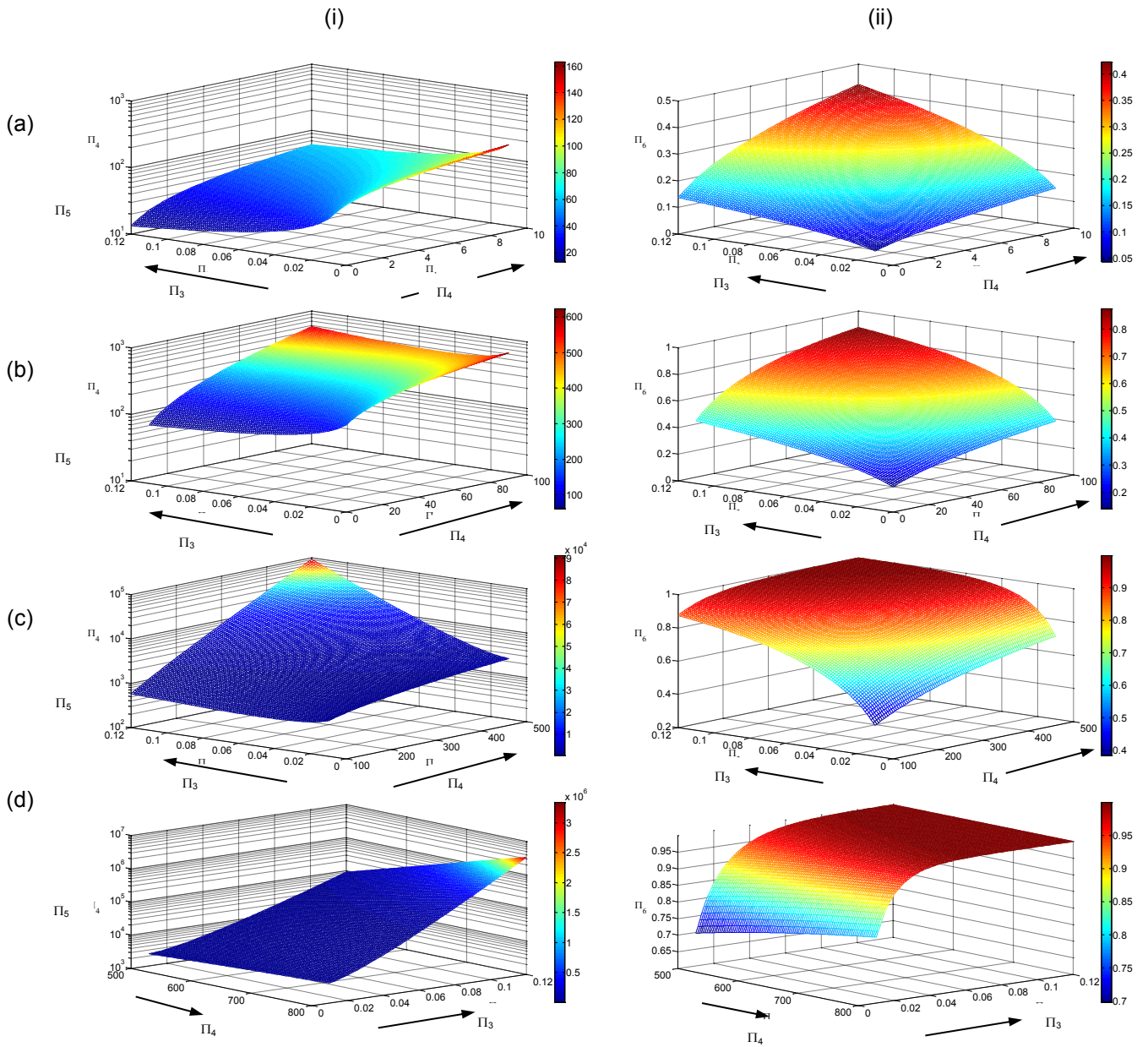


Figure 9: Variation of (i) Π_5 (note log scale) and (ii) Π_6 with Π_3 and Π_4 : (a – d) denote different ranges of cleaning cost, Π_4 . Arrows indicate scale direction.

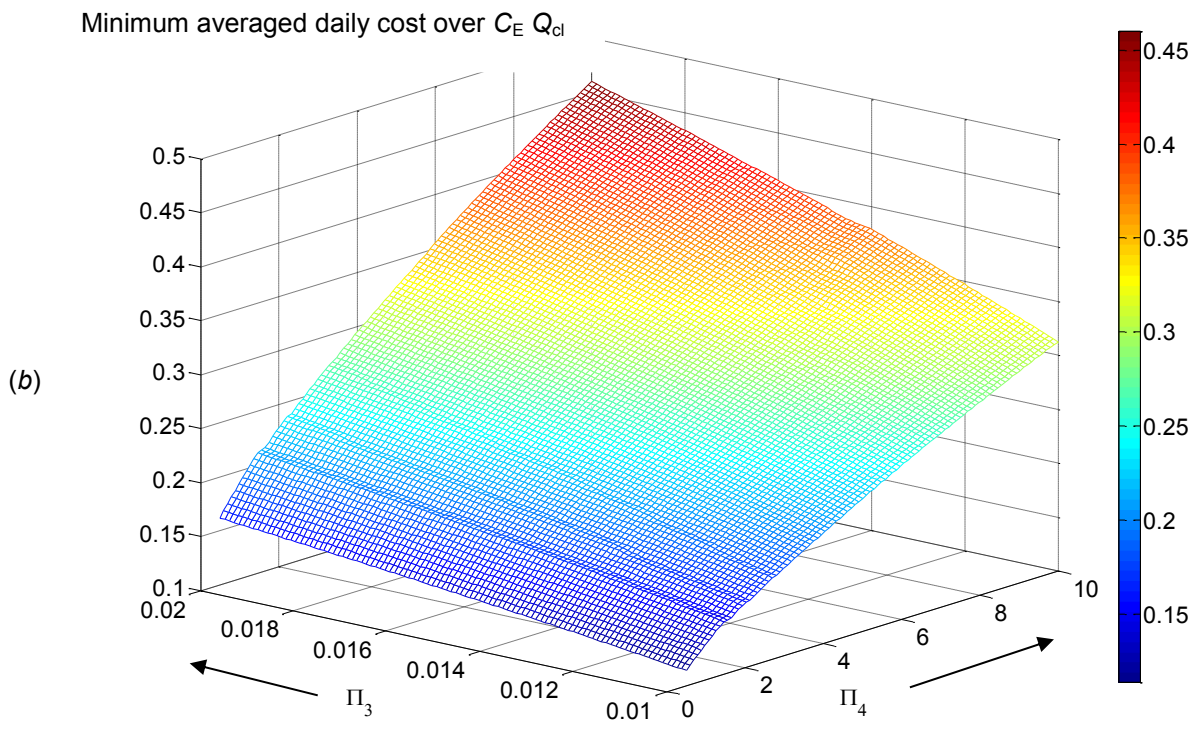
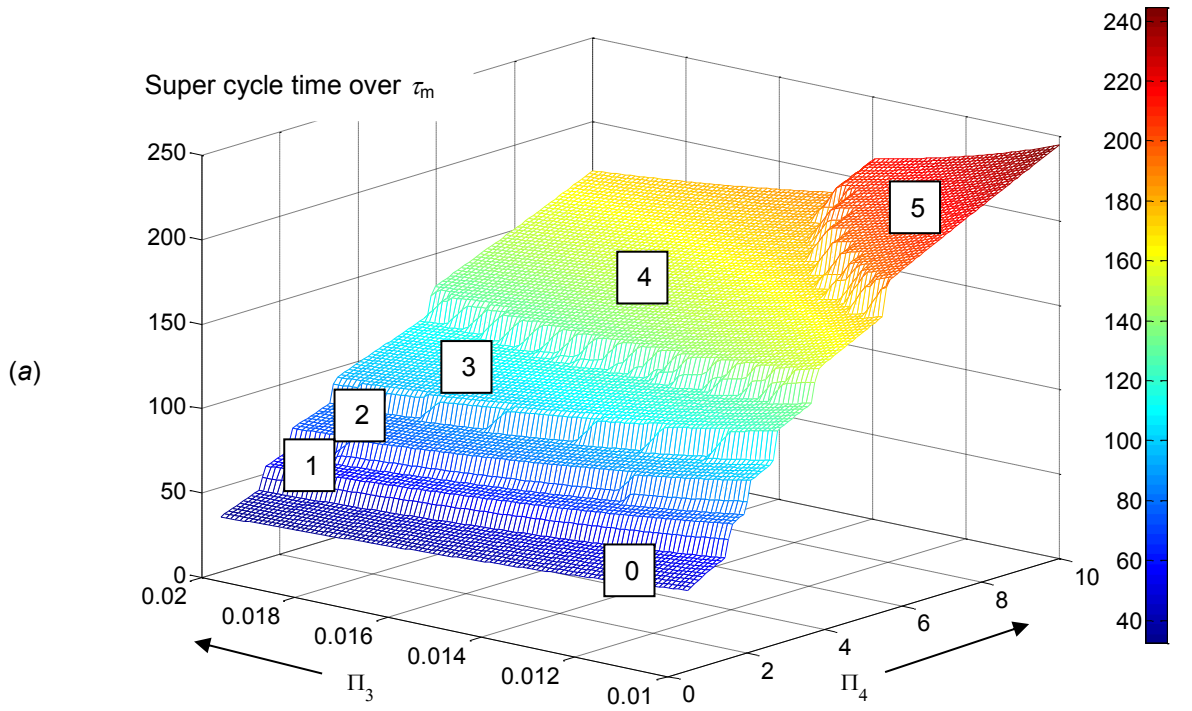
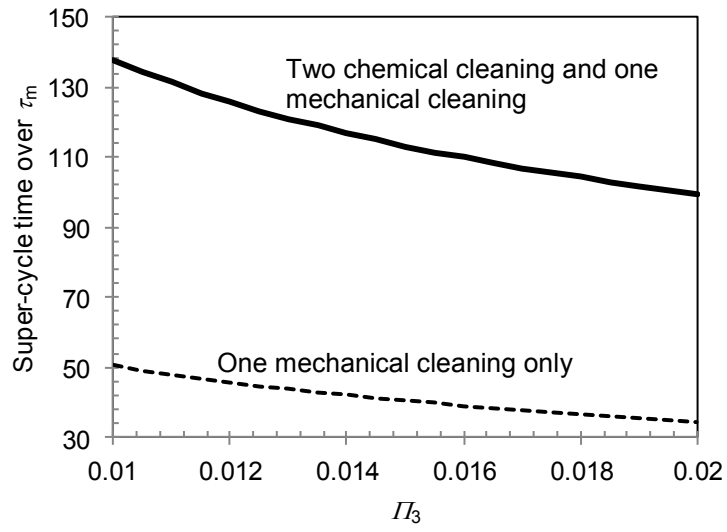


Figure 10: Variation in dimensionless (a) super-cycle time and (b) cost under a range of fouling rates (Π_3) and mechanical cleaning cost (Π_4).

(a)



(b)

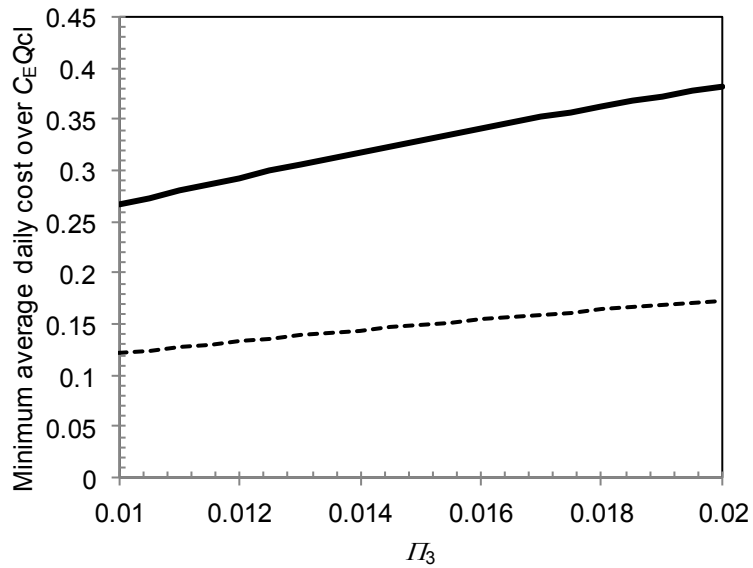


Figure 11 Effect of (dimensionless) fouling rate Π_3 on optimal super-cycle (a) length and (b) time-averaged cost for the exchanger in Figure 10 under 'reactive' (dashed locus, $\Pi_4 = 0.67$) and 'proactive' (solid locus, $\Pi_4 = 6.67$) cleaning strategies. Other parameters summarised in Table 8.



Edward Ishiyama is a senior research analyst at IHS (Downstream Research), London, and also an embedded researcher at the Department of Chemical Engineering and Biotechnology, University of Cambridge, UK. His current research includes applying heat transfer, process control, and thermodynamic principles to identify and solve problems associated with heat exchangers undergoing fouling. He holds a Ph.D. degree from the University of Cambridge, UK.



Bill Paterson has retired from a senior lectureship at Cambridge and a fellowship at Wolfson College, having previously served at the universities of Edinburgh, Queensland, Adelaide, and Canterbury (NZ), and having been a Development Manager at ICI Petrochemicals Division. He holds a B.Sc. and Ph.D. from Edinburgh. His research interests have mainly involved process systems and simulation, reaction engineering, and heat transfer. In particular, he still pursues his interests in the fouling and cleaning of heat transfer surfaces.



Ian Wilson is a Reader in the Department of Chemical Engineering and Biotechnology at the University of Cambridge. He holds degrees in chemical engineering from Cambridge and the University of British Columbia. He is a Fellow of Jesus College, Cambridge. His main research interests are in the rheology and processing of soft solids, heat exchanger fouling and cleaning, and food processing.